

# *In silico* modeling of $\alpha$ -glucosidase, aldose reductase, and PPAR- $\gamma$ with benzoyl/sulfonyl hydrazone derivatives using molecular docking, ADMET, and molecular dynamics simulations

Gizem TATAR YILMAZ<sup>1\*</sup> , Bedriye Seda KURŞUN AKTAR<sup>2</sup> , Emine Elçin ORUÇ-EMRE<sup>3</sup> 

<sup>1</sup> Department of Biostatistics and Medical Informatics, Faculty of Medicine, Karadeniz Technical University, Trabzon, Türkiye.

<sup>2</sup> Department of Hair Care and Beauty Services, Yeşilyurt Vocational School, Malatya Turgut Özal University, Malatya, Türkiye

<sup>3</sup> Department of Chemistry, Faculty of Arts and Sciences, Gaziantep University, Gaziantep, Türkiye

\* Corresponding Author. E-mail: [gizemtatar@gmail.com](mailto:gizemtatar@gmail.com) (G.T.Y); Tel. +90 462 377 53 07.

Received: 25 December 2022/ Revised: 17 March 2023 / Accepted: 17 March 2023

## ABSTRACT:

Type 2 diabetes mellitus (T2DM) is the most common type of diabetes and has become a serious public health problem in over the world. There are various antidiabetic drugs on the market, but most of these drugs cause many side effects such as diarrhea, kidney failure, musculoskeletal pain, and enlarged urinary system infections in the clinical treatment of T2DM. Therefore, there is a need for new antidiabetic drugs that can be used orally, are safe with improved efficacy, and reduced side effects. Today, drugs targeting alpha-glucosidase ( $\alpha$ -glucosidase), peroxisome proliferator activating receptor gamma (PPAR- $\gamma$ ), and aldose reductase have an important role in the treatment of T2DM. This study is aimed to develop new antidiabetic agents with molecular modeling methods that are more effective, and specific and have fewer side effects than existing drug molecules for  $\alpha$ -glucosidase, PPAR- $\gamma$ , and aldose reductase. Herein, enzyme-ligand interaction mechanisms between target enzymes and 45 hydrazone compounds were examined by using molecular docking and molecular dynamics simulation methods. In addition, the ADME properties of these compounds and their pharmacokinetic suitability according to Lipinski and Veber's rules were evaluated. Compound 2 has shown the best binding affinity against  $\alpha$ -glucosidase, compound 27 for aldose reductase, and compound 4 for PPAR- $\gamma$  and these compounds exhibited good ADME properties. Also, the best active hydrazone compounds have been observed to interact with key amino acid residues on target enzymes via hydrogen bonds. This information can guide the development of new antidiabetic agents by making important contributions to experimental studies.

**KEYWORDS:** T2DM; hydrazone; ADME; molecular docking; molecular dynamics simulation

## 1. INTRODUCTION

Diabetes mellitus is a chronic disease that is rapidly increasing all over the world. There are 463 million patients in the world in 2019, and this number is expected to reach 578 million in 2030 and 700 million in 2045. Type 2 diabetes mellitus (T2DM) is the most common class, making up approximately 90% of all diabetes cases in over the world [1,2]. Oral antidiabetic drugs used in the treatment of Type 2 diabetes are drugs that regulate the secretion of insulin from the pancreas in the body and/or the effect of insulin on target cells or slow down the absorption of glucose from the intestine [3,4]. The target of oral antidiabetic drugs used in the clinic; is to reduce insulin resistance, regulate hyperglycemia control, provide metabolic control, and improve the quality of life of diabetic patients.

Peroxisome proliferator activating receptors (PPARs) are ligand-dependent transcription factors responsible for the regulation of lipid and glucose metabolism [5]. Thiazolidinediones (TZD) exert an agonistic effect by activating PPAR- $\gamma$ , which has a role in lipid metabolism. These drugs increase the effect of insulin while reducing glucose and free fatty acid levels. As with biguanides, thiazolidinediones do not cause hypoglycemia when used alone. When used alone or in combination with therapy, it causes weight gain and may cause peripheral edema. Congestive heart failure, elevation in liver enzymes, and LDL cholesterol are the

**How to cite this article:** Tatar Yılmaz G, Kurşun Aktar BS, Oruç-Emre EE. *In silico* modeling of  $\alpha$ -glucosidase, aldose reductase, and PPAR- $\gamma$  with benzoyl/sulfonyl hydrazone derivatives using molecular docking, ADMET, and molecular dynamics simulations. J Res Pharm. 2023; 27(4): 1567-1576.

side effects. Drugs included in this group such as rosiglitazone and pioglitazone are used in the treatment (Figure 1) [3,4].

Moreover, aldose reductase is known to play a critical role in the cardiovascular, renal, ocular system, and nerve neuropathies in diabetic patients. Because it has been found that aldose reductases accumulate in tissues where diabetic complications occur such as the retina, nerve tissues, kidney, and aorta [6]. In addition,  $\alpha$ -glucosidase enzymes such as glucoamylase, sucrase, maltase, isomaltase, and lactase in the small intestine are enzymes responsible for the breakdown of complex carbohydrates such as oligo and disaccharides into monosaccharides. Monosaccharides are absorbed from the intestinal wall and pass into the blood. These enzyme inhibitors slow down glucose absorption by competitively inhibiting  $\alpha$ -glucosidase enzymes. In this way, they indirectly prevent hyperglycemia. In treatment, a drug called acarbose is used to slow down glucose absorption. Elevated liver enzymes and gastrointestinal side effects are observed [3,4].

While most of the antidiabetic drugs currently used in treatment cause many side effects such as diarrhea, liver diseases, respiratory system infections kidney failure urinary system infections, and musculoskeletal pain, they fail to control the targeted plasma glucose levels in some patients [7,8]. These side effects increase even more when switching to 2 or 3 drug combinations. Therefore, there is a need for new antidiabetic drugs that can be used orally, safely, with improved efficacy and reduced side effects.

The benzoyl/sulfonyl hydrazone compounds have many different pharmacological activities such as antidiabetic [9], antioxidant, antiviral [10], analgesic [11], antiepileptic [12], anti-inflammatory [13], antimicrobial [14], and, anticancer [15]. Thus, the activities of previously synthesized benzoyl/sulfonyl hydrazones against  $\alpha$ -glucosidase, aldose reductase, and PPAR- $\gamma$  enzymes were investigated by *in silico* molecular modeling in this study [16-18].

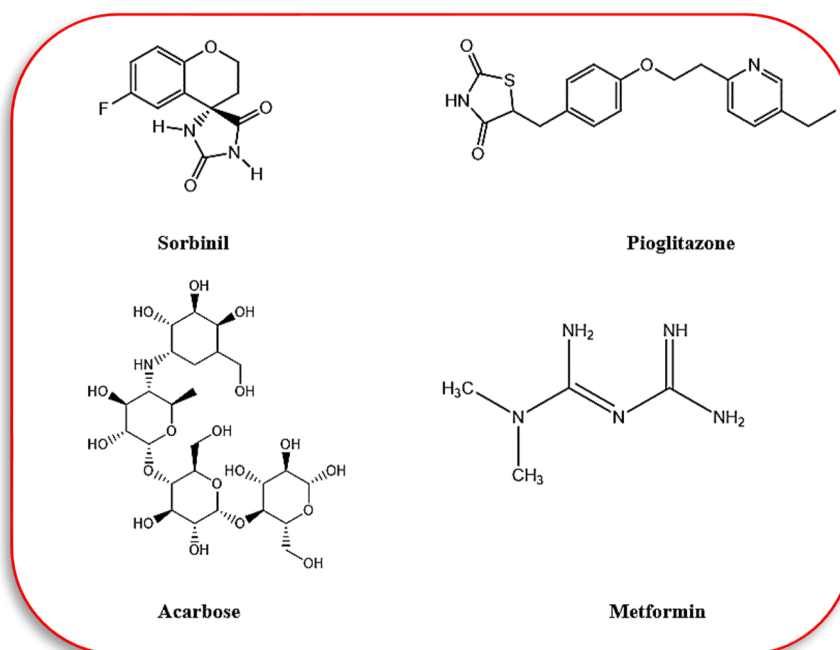


Figure 1. The antidiabetic drugs.

## 2. RESULTS and DISCUSSION

### 2.1 Molecular Docking Simulation

In order to clarify the binding mechanism and affinities of the benzoyl/sulfonyl hydrazone compounds in the active site of  $\alpha$ -glucosidase, aldose reductase, and PPAR- $\gamma$  were investigated by molecular docking approach. The **compound 1-45** were docked into the binding pocket site of the target enzyme and calculated binding energies (kcal/mol) (**Table 2**).  $\alpha$ -Alpha-glucosidase is an important promising target for the treatment of obesity and diabetes [19,20]. According to this docking study results, **compound 2** showed the best binding affinity against  $\alpha$ -glucosidase compared with the reference compound (acarbose). The most active **compound**

**2** interacted with residues Arg600, Gly651, Leu650, Asp518, Asp282, Met519, Leu677, Leu678 and Trp481 in the  $\alpha$ -glucosidase binding pocket site. This compound showed hydrogen bond interactions with Arg600, Gly651, Leu650, Asp518, also Leu677 and Leu678 made an alkyl and  $\pi$ -alkyl interaction (**Figure 2**).

**Table 1.** Chemical structures of benzoyl/sulfonyl hydrazone derivatives (1-45).

1. R <sub>4</sub> =H	13. R <sub>4</sub> = H	26. R <sub>4</sub> = H	36. R <sub>4</sub> = H
2. R <sub>4</sub> =Cl	14. R <sub>4</sub> = Br	27. R <sub>4</sub> = Br	37. R <sub>4</sub> = Br
3. R <sub>4</sub> =F	15. R <sub>4</sub> = Cl	28. R <sub>4</sub> = Cl	38. R <sub>4</sub> = Cl
4. R <sub>4</sub> =NO <sub>2</sub>	16. R <sub>4</sub> = F	29. R <sub>4</sub> = F	39. R <sub>4</sub> = F
5. R <sub>3</sub> = CF <sub>3</sub>	17. R <sub>4</sub> = OCH <sub>3</sub>	30. R <sub>4</sub> = OCH <sub>3</sub>	40. R <sub>4</sub> = OCH <sub>3</sub>
6. R <sub>4</sub> =CF <sub>3</sub>	18. R <sub>4</sub> = NO <sub>2</sub>	31. R <sub>4</sub> = CH <sub>3</sub>	41. R <sub>4</sub> = CH <sub>3</sub>
7. R <sub>2</sub> = F, R <sub>4</sub> =CF <sub>3</sub>	19. R <sub>2</sub> = CF <sub>3</sub>	32. R <sub>4</sub> = NO <sub>2</sub>	42. R <sub>4</sub> = NO <sub>2</sub>
8. R <sub>2</sub> = F, R <sub>5</sub> =CF <sub>3</sub>	20. R <sub>3</sub> = CF <sub>3</sub>	33. R <sub>2</sub> = OCF <sub>3</sub>	43. R <sub>2</sub> = OCF <sub>3</sub>
9. R <sub>4</sub> = OCF <sub>3</sub>	21. R <sub>4</sub> = CF <sub>3</sub>	34. R <sub>3</sub> = OCF <sub>3</sub>	44. R <sub>3</sub> = OCF <sub>3</sub>
10. R <sub>4</sub> = SCH <sub>3</sub>	22. R <sub>3</sub> = CF <sub>3</sub> , R <sub>5</sub> = CF <sub>3</sub>	35. R <sub>4</sub> = OCF <sub>3</sub>	45. R <sub>4</sub> = OCF <sub>3</sub>
11. R <sub>4</sub> = SCF <sub>3</sub>	23. R <sub>2</sub> = OCF <sub>3</sub>		
12. isoniazid	24. R <sub>3</sub> = OCF <sub>3</sub>		
	25. R <sub>4</sub> = OCF <sub>3</sub>		

Docking studies for aldose reductase revealed that all compounds showed better docking binding affinities compared with the reference compound (sornibil). Especially, **compounds 27, 28, 31, and 32** showed very strong binding affinity against aldose reductase enzyme with binding energy (-10.59, -10.56, -10.47, and -10.41 kcal/mol, respectively) (**Table 2**). The Br atom of the most active **compound 27**, had alkyl bond interaction with Cys303 and Pro310, and this compound formed  $\pi$ - $\pi$ -pi stacked with Trp20, Trp111, Val47, and alkyl bond with Cys298, and Leu300 (**Figure 2**). The other active compounds showed similar binding sites.

The docking studies of compounds revealed that **compounds 4 and 32** showed a good binding affinity with significant binding interaction with key residues of PPAR- $\gamma$  (**Figure 2**). Compound **4** displayed strong hydrogen bond interactions with Leu228 (1.79 Å), Lys367 (1.88 Å), His449 (1.93 Å), also alkyl bond with Pro227, Ala292, Ile326, and  $\pi$ -alkyl bond Cys285 and Lys367. Further, **compound 32** exhibited six hydrogen bonds with Leu 228, Lys367, Cys285, Pro227, Ser289, and His449. Similar to **compound 4**, **compound 32** formed an alkyl bond with Pro227, Ala292, Ile326, and  $\pi$ -alkyl bond Met364 (**Figure 2**).

**Table 2.** The lowest binding energy values of the 45 benzoyl/sulfonyl hydrazone compounds and reference compounds from each docking analysis in the active site of  $\alpha$ -glucosidase, aldose reductase, and PPAR- $\gamma$ .

	PPAR-gamma	Aldose reductase	Alpha-glucosidase
Compound number	Binding energy (kcal/mol)	Binding energy (kcal/mol)	Binding energy (kcal/mol)
Reference compounds	-8.19 (Pioglitazone)	-6.41 (Sorbinitol)	-4.66 (Acarbose)
1	-7.98	-9.26	-7.47
2	-8.30	-9.63	-7.62
3	-7.97	-8.71	-7.44
4	-9.30	-8.84	-6.55
5	-8.31	-9.54	-5.78
6	-7.94	-9.68	-5.89
7	-7.82	-9.15	-5.39
8	-8.15	-9.72	-6.64
9	-8.17	-9.00	-6.25
10	-8.33	-9.74	-7.38
11	-8.45	-8.79	-5.23
12	-7.56	-8.94	-7.23
13	-6.74	-7.40	-6.79
14	-7.06	-8.10	-7.42
15	-6.91	-7.99	-7.28
16	-6.63	-7.39	-6.88
17	-6.92	-7.60	-6.83
18	-7.81	-8.11	-6.52
19	-6.91	-7.84	-6.73
20	-6.70	-7.62	-7.14
21	-6.56	-7.48	-6.38
22	-6.87	-7.24	-7.21
23	-6.38	-7.30	-6.76
24	-6.70	-7.53	-6.83
25	-6.80	-7.18	-6.65
26	-8.29	-10.16	-6.84
27	-8.83	-10.59	-6.81
28	-8.53	-10.56	-6.58
29	-8.06	-9.99	-6.58
30	-8.47	-9.86	-6.90
31	-8.52	-10.47	-6.86
32	-9.26	-10.41	-7.04
33	-8.59	-9.23	-6.97
34	-8.69	-9.94	-6.98
35	-8.25	-9.93	-6.36
36	-8.20	-9.43	-6.28
37	-7.89	-10.03	-6.43
38	-7.65	-9.70	-6.57
39	-7.78	-9.05	-6.20
40	-8.46	-9.41	-6.94
41	-8.08	-9.50	-6.26
42	-8.07	-9.61	-7.36
43	-8.10	-8.97	-5.66
44	-7.97	-9.52	-6.49
45	-7.23	-9.53	-5.95

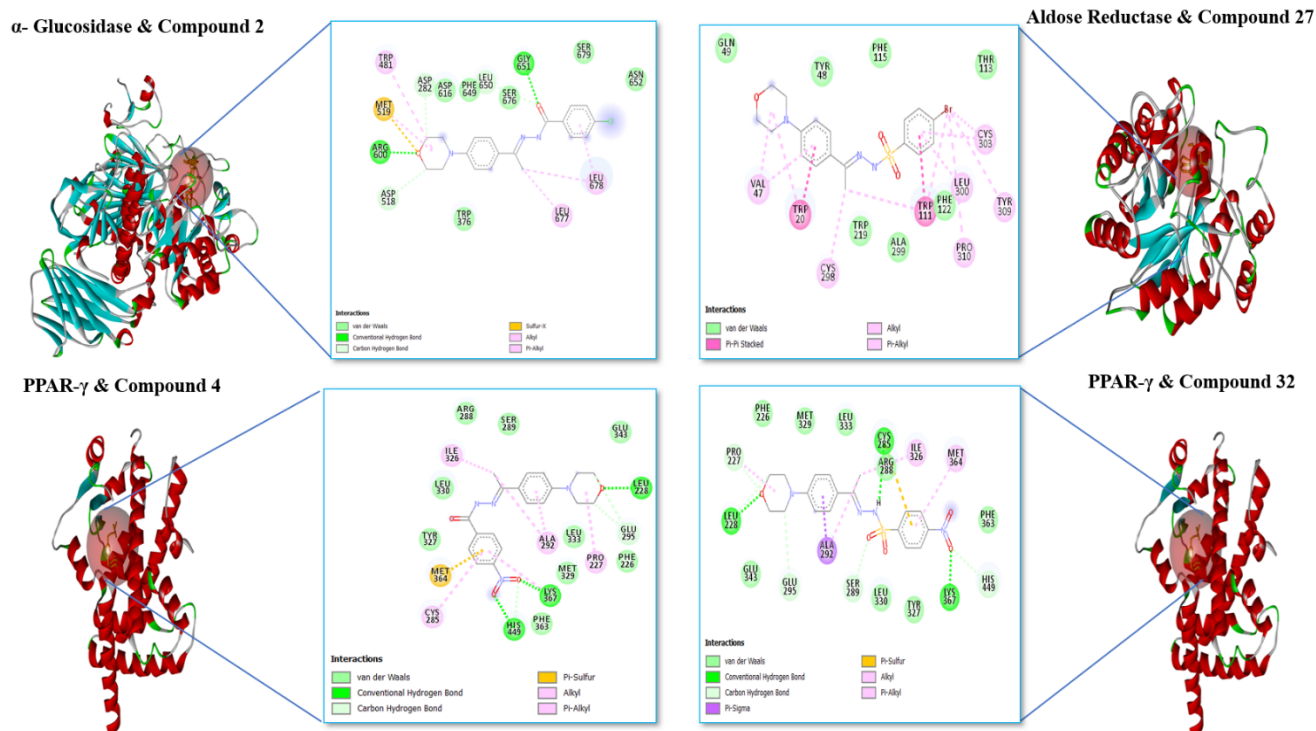


**Figure 2.** Molecular docking simulations analysis of the lowest energy binding conformations of alpha-glucosidase, aldose reductase, and PPAR- $\gamma$  with the most potent compounds is given.

## 2.2 ADME and Toxicity

Pharmacokinetic properties of the compounds such as absorption, distribution, metabolism, elimination, and toxicity (ADME+T) were calculated by in silico methods. All analyzed compounds were observed to bind poorly to carrier plasma proteins in the blood, except compounds **19**, **20**, and **21**. In addition, compounds **5**, **6**, and **19** are toxic to the liver according to their hepatotoxicity values. Also, all compounds have good intestinal absorption levels. However, compounds **43**, **44**, and **45** also have poor intestinal absorption levels. Besides, all studied compounds have PSA values less than 140 Å and AlogP98 values less than 5, except for compounds **19**, **20**, and **21**. Furthermore, compounds **43**, **44**, and **45** fall outside the ADME model ellipse filter, indicating poor intestinal absorption and BBB penetration ability. In addition, all compounds except compounds **1**, **4**, and **18** did not exhibit mutagenicity as predicted by the TOPKAT Ames mutagenicity test of Discovery Studio 2020 Client [21] (see **Figure 3** and **Supplementary material in Table S1**).

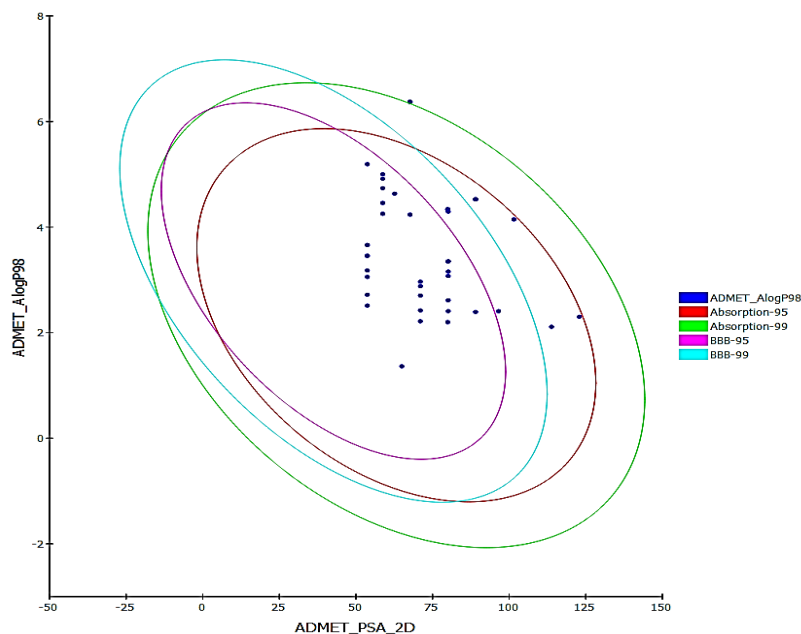


**Figure 3.** The plot of ADMET for compounds (1-45) showing the 95% and 99% confidence limit ellipses corresponding to the blood barrier (BBB) and intestinal absorption.

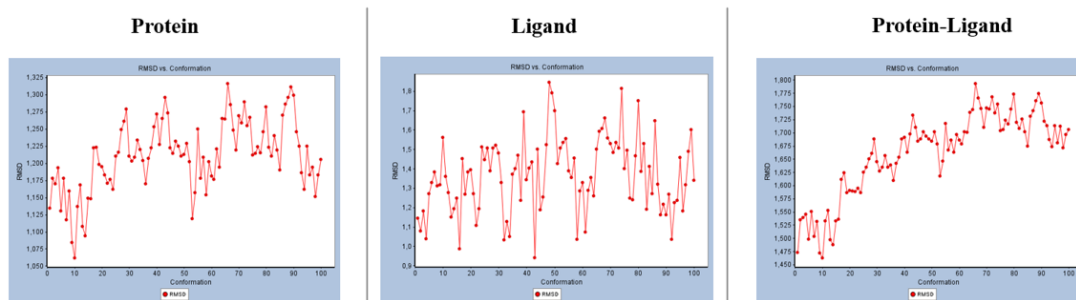
### 2.3 Molecular Dynamic Simulations

Molecular dynamic simulation is applied to construct a realistic model of a structure's motion, perform conformational searching, produce time series analysis of structural and energetic properties, understand protein-ligand structure stability, and analyze solvent effects. Accordingly, we performed the molecular dynamic simulation for the target enzymes with the most potent compounds. The non-covalent interaction analysis, RMSF, RMSD, and the average of total energy for each structure were calculated during the MD simulation (see Figure 4-6).

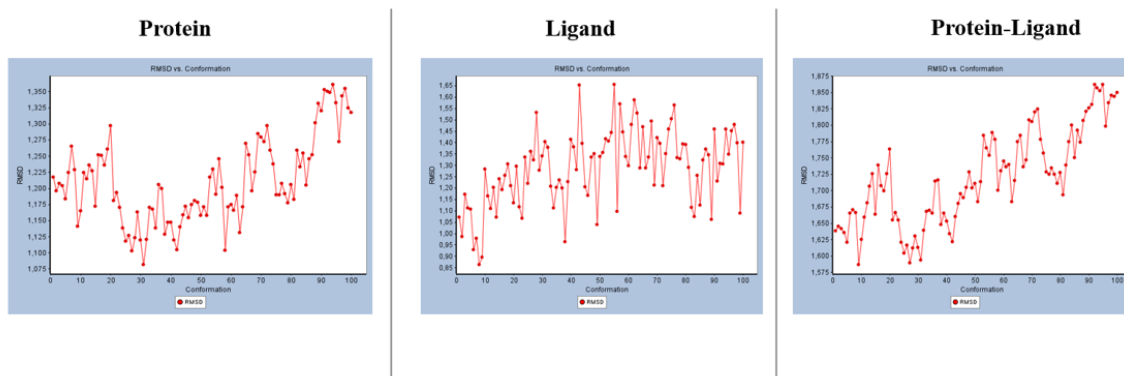
Our analyses indicated that **compound 2**, which is the most effective compound against alpha-glucosidase according to molecular docking analysis, continued to interact with Leu650, Asp518, Leu677, Leu678, and Trp481 of alpha-glucosidase during the MD simulation. In addition, **compound 27**, which has a very strong effect against aldose reductase enzyme with -10.59 kcal/mol binding energy, established new non-covalent interactions with Gln49, Trp219, Phe122, Phe115, Phe121, and His306 after MD simulation. Also, the interaction between Leu300 of aldose reductase and compound 27 became stronger (bond length: 4.37 to 2.09) after the MD simulation. Likewise, the interaction between the Met364, Pro227, Ala292, Ile326, and Cys285 of PPAR- $\gamma$  and **compound 4**, continued to interact steadily during the MD simulation (see Supplementary Material Figure S1). The results of this analysis showed that these important contacts were preserved in the protein-ligand compounds.

Furthermore, the RMSD values of backbone C $\alpha$  atoms were calculated to be in the range of 0.85 to 2.05 Å, for protein-ligand complex, protein, and ligand structures conformation during the MD simulation (see Figure 4). Besides, it was observed that the RMSF values of residues of protein range from 0.25 to 2.75 Å (see Figure 5). The total energy values ranged from -170.250 to -169.000 kcal/mol for the alpha-glucosidase and compound 2, -74.700 to -73.900 kcal/mol for the aldose reductase and compound 27, -65.300 to -64.600 for the PPAR- $\gamma$  and compound 4 (Figure 6).

*Alpha-glucosidase & Compound 2*



*Aldose Reductase & Compound 27*



*PPAR- $\gamma$  & Compound 4*

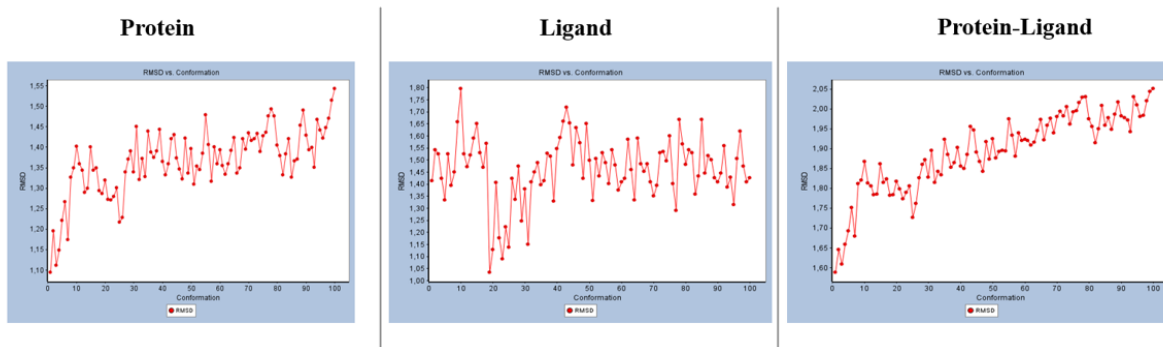


**Figure 4.** The RMSD trajectory of protein, ligand, and protein-ligand complex structures during the 225ps MD simulation time

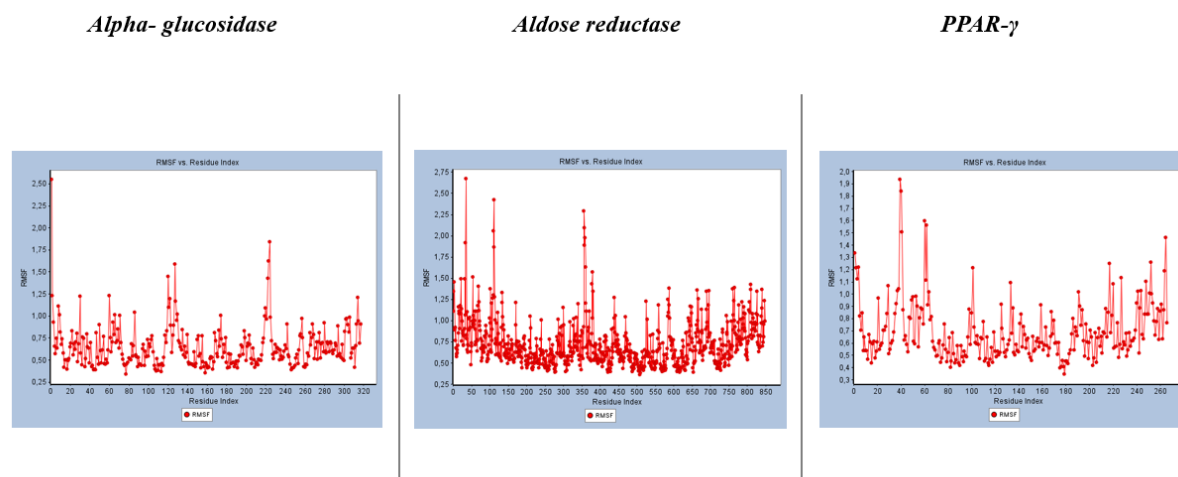


Figure 5. The RMSF profile of alpha-glucosidase, aldose reductase, and PPAR- $\gamma$  in the complex structures.

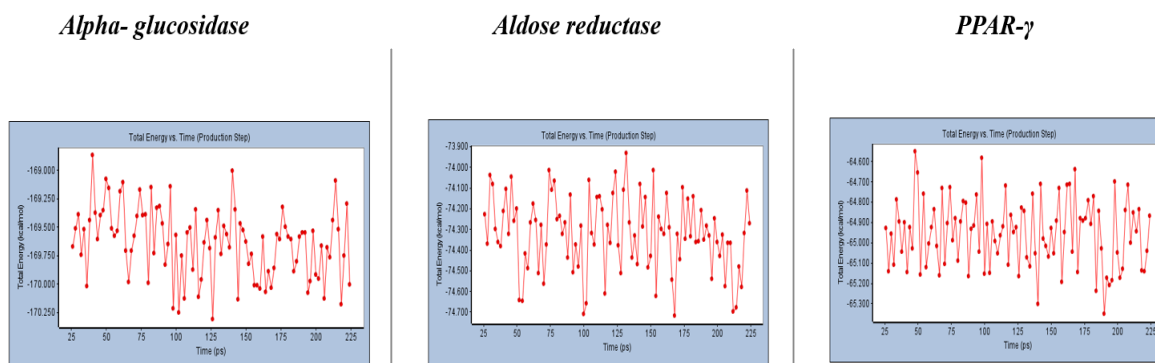


Figure 6. The total energy trajectory of alpha-glucosidase, aldose reductase, and PPAR- $\gamma$  with the most potent compounds at the phase (225 ps) in the simulation.

### 3. CONCLUSION

In conclusion, this study explains the antidiabetic activity of benzoyl/sulfonyl hydrazone by molecular modeling methods. The results revealed that **compound 2** showed the best binding affinity to  $\alpha$ -glucosidase, **compound 27** for aldose reductase, and **compound 4** for PPAR- $\gamma$ , and these compounds exhibited good ADME properties. In addition, molecular dynamics simulation studies have shown that the best active hydrazone compounds have stable non-covalent interactions with key amino acid residues on target enzymes. Therefore, these findings would be useful for further experimental studies with target enzymes. Thus, by examining the pharmacokinetic and pharmacodynamic analyzes of these compounds for  $\alpha$ -glucosidase, PPAR- $\gamma$ , and aldose reductase enzymes, which play a critical role in the treatment of T2DM, with molecular modeling methods in a more advantageous way in terms of time and cost, it will enable more reliable and economical experimental studies.

### 4. MATERIALS AND METHODS

#### 4.1 Molecular docking

Molecular docking, known as structure-based drug design, is a computer-assisted drug design method that allows examining the interactions between target biomolecules with 3-dimensional (3D) structure information and effector structures. It is used to predict the preferred orientation of one of the two molecules that bind together to form a stable complex, thus predicting the affinity of small molecule drug candidates towards protein targets, their binding to these macromolecules, and thus their biological activity.

In line with this information, molecular docking analysis was applied to elucidate the interaction mechanisms between the 3-dimensional structure of  $\alpha$ -glucosidase, aldose reductase, and PPAR- $\gamma$  target enzymes and 45 compounds and to evaluate their biological activities. The 3-dimensional crystal structures of these enzymes were accessed from the RSCB protein database (<https://www.rcsb.org/>). The lowest resolution human species with PDB codes 5NN4 for  $\alpha$ -glucosidase, 4LBS for aldose reductase, and 6MS7 for PPAR- $\gamma$  were used. Then, the active sites of these target enzymes were determined and the molecular docking process with 45 compounds (see in Figure) was carried out with the AutoDock 4.2 [22] program. Then, molecular docking was performed with the Lamarckian Genetic Algorithm with 100 run steps so that the compounds can be flexibly bounded to the active site of the target enzyme structures. As a result of this analysis, the binding free energy ( $\Delta G$ ) and binding constant ( $K_i$ ) was calculated for each possible conformational state. The 2D binding analyses of enzyme-ligand structures with the lowest energy conformation were performed with the BIOVIA Discovery Studio 2020 Client [21].

#### 4.2 ADME and Toxicity Analysis

The Absorption, Distribution, Metabolism, Excretion, and Toxicity (ADMET) properties of analyzed compounds were examined by using ADMET descriptors of BIOVIA Discovery Studio 2020 Client. These descriptors including Aqueous Solubility, Blood Brain Barrier (BBB) penetration, Cytochrome P450 2D6 (CYP2D6) binding, Hepatotoxicity, Intestinal Absorption, Plasma protein binding (PPB) were calculated for ligands. Further, the analyzed compounds were subjected to Ames mutagenicity test of BIOVIA Discovery Studio 2020 Client [21] with TOPKAT (Toxicity Prediction by Computer Assisted Technology) protocol. The Ames test is a widely used biological test to understand the mutagenic potential of chemical compounds.

#### 4.3 Molecular Dynamics Simulations

This analysis was performed for the most effective binding compounds and target enzymes using the NAMD module of BIOVIA Discovery Studio [21]. In this study, we used the more realistic explicit periodic boundary solvation model of water to observe significant structural transitions. We performed the standard dynamics cascade protocol, which combines the following defined simulation procedures after the solvation processes. After solving, the standard dynamic cascade protocol combining the following defined simulation procedures was performed. After solving, the standard dynamic cascade protocol combining the following defined simulation procedures was performed. An initial minimization step was performed with the 1000-step steepest descent algorithm, followed by a 2000-step conjugate gradient, to provide a low-energy starting point for the dynamic stages. With the heating and balancing phase, the energy in the system is properly distributed between all degrees of freedom and the system kept the temperature of the entire protein-ligand system at the target temperature (300 K). A molecular dynamics generation run at 200 picoseconds (ps) simulation time was performed NPT ensemble at a given temperature and pressure, based on the equilibrated system from the previous step. To investigate the stability of the entire protein-ligand complex, a set of trajectories analyzing parameters including root mean square derivation (RMSD), and root mean square fluctuation (RMSF) profile, were estimated from all MD simulation run.

**Acknowledgements:** This work was supported by Çankırı Karatekin University Scientific Research Projects Governing Unit (BAPYB) (Grant no: YM0150219B14, Çankırı, Türkiye) and Gaziantep University Scientific Research Projects Governing Unit (BAPYB) (Grant no: FEF.14.01, Gaziantep, Türkiye) The numerical calculations reported in this abstract were performed at The Scientific and Technological Research Council of Turkey (TUBITAK) ULAKBIM High Performance and Grid Computing Center (TRUBA resources).

**Author contributions:** Concept – B. S. K. A., E. E. O. E.; Design – B. S. K. A., E. E. O. E.; Supervision – G. T. Y., B. S. K. A., E. E. O. E.; Resources – G. T. Y., B. S. K. A., E. E. O. E.; Materials – B. S. K. A.; Data Collection and/or Processing – G. T. Y., B. S. K. A.; Analysis and/or Interpretation – G. T. Y.; Literature Search – G. T. Y., B. S. K. A.; Writing – G. T. Y., B. S. K. A., E. E. O. E.; Critical Reviews – G. T. Y., B. S. K. A., E. E. O. E.

**Conflict of interest statement:** The authors declared that they have no conflict of interest.

## REFERENCES

- [1] Fang Y, Xu J, Li Z, Yang Z, Xiong L, Jin Y, Qin W, Xie S, Zhu W, Chang S. Design and synthesis of novel pyrimido[5,4-d]pyrimidine derivatives as GPR119 agonist for treatment of type 2 diabetes. *Bioorg Med Chem.* 2018;26(14):4080-4087. <https://doi.org/10.1016/j.bmc.2018.06.035>
- [2] Home, Resources, diabetes L with, Acknowledgement, FAQs, Contact, vd. 9th edition | IDF Diabetes Atlas. <https://diabetesatlas.org/atlas/ninth-edition/> (accessed December 23, 2022)
- [3] Liu Z, Yang B. Drug development strategy for Type 2 Diabetes: Targeting positive energy balances. *Curr Drug Targets.* 2019;20(8):879-890. <https://doi.org/10.2174/1389450120666181217111500>
- [4] Wang Y, Perri M. A systematic review of patient-reported satisfaction with oral medication therapy in patients with Type 2 Diabetes. *Value Health.* 2018;21(11):1346-1353. <https://doi.org/10.1016/j.jval.2018.05.001>
- [5] Chinetti G, Fruchart JC, Staels B. Peroxisome proliferator-activated receptors (PPARs): Nuclear receptors at the crossroads between lipid metabolism and inflammation. *Inflamm Res.* 2000;49(10):497-505. <https://doi.org/10.1007/s000110050622>
- [6] Oates PJ, Mylari BL. Aldose reductase inhibitors: therapeutic implications for diabetic complications. *Expert Opin Investig Drugs.* 1999;8(12):2095-2119. <https://doi.org/10.1517/13543784.8.12.2095>
- [7] Kang SU. GPR119 agonists: a promising approach for T2DM treatment? A SWOT analysis of GPR119. *Drug Discov Today.* 2013;18(23-24):1309-1315. <https://doi.org/10.1016/j.drudis.2013.09.011>
- [8] Ohishi T, Yoshida S. The therapeutic potential of GPR119 agonists for type 2 diabetes. *Expert Opin Investig Drugs.* 2012;21(3):321-328. <https://doi.org/10.1016/j.drudis.2013.09.011>
- [9] Imran S, Taha M, Ismail NH, Kashif SM, Rahim F, Jamil W, Hariono M, Yusuf M, Wahab H. Synthesis of novel flavone hydrazones: In-vitro evaluation of  $\alpha$ -glucosidase inhibition, QSAR analysis and docking studies. *Eur J Med Chem.* 2015;105:156-170. <https://doi.org/10.1016/j.ejmech.2015.10.017>
- [10] El-Sabbagh OI, Rady HM. Synthesis of new acridines and hydrazones derived from cyclic  $\beta$ -diketone for cytotoxic and antiviral evaluation. *Eur J Med Chem.* 2009;44(9):3680-3686. <https://doi.org/10.1016/j.ejmech.2009.04.001>
- [11] Sondhi SM, Dinodia M, Kumar A. Synthesis, anti-inflammatory and analgesic activity evaluation of some amidine and hydrazone derivatives. *Bioorg Med Chem.* 2006;14(13):4657-4663. <https://doi.org/10.1016/j.bmc.2006.02.014>
- [12] Sridhar SK, Pandeya SN, Stables JP, Ramesh A. Anticonvulsant activity of hydrazones, Schiff and Mannich bases of isatin derivatives. *Eur J Pharm Sci.* 2002;16(3):129-132. [https://doi.org/10.1016/s0928-0987\(02\)00077-5](https://doi.org/10.1016/s0928-0987(02)00077-5)
- [13] Vasantha K, Basavarajaswamy G, Vaishali Rai M, Boja P, Pai VR, Shruthi N, Bhat M. Rapid 'one-pot' synthesis of a novel benzimidazole-5-carboxylate and its hydrazone derivatives as potential anti-inflammatory and antimicrobial agents. *Bioorg Med Chem Lett.* 2015;25(7):1420-1426. <https://doi.org/10.1016/j.bmcl.2015.02.043>
- [14] Angelova VT, Valcheva V, Vassilev NG, Buyukliev R, Momekov G, Dimitrov I, Saso L, Djukic M, Shivachev B. Antimycobacterial activity of novel hydrazide-hydrazone derivatives with 2H-chromene and coumarin scaffold. *Bioorg Med Chem Lett.* 2017;27(2):223-227. <https://doi.org/10.1016/j.bmcl.2016.11.071>
- [15] Liu WY, Li HY, Zhao BX, Shin DS, Lian S, Miao JY. Synthesis of novel ribavirin hydrazone derivatives and anti-proliferative activity against A549 lung cancer cells. *Carbohydr Res.* 2009;344(11):1270-1275. <https://doi.org/10.1016/j.carres.2009.05.017>
- [16] Aktar BSK, Sicak Y, Tok TT, Oruç EEE, Yağlıoğlu AŞ, İyidoğan AK, Öztürk M, Demirtaş I. Designing heterocyclic chalcones, benzoyl/sulfonyl hydrazones: An insight into their biological activities and molecular docking study. *J Mol Struct.* 2020; 1211: 128059. <https://doi.org/10.1016/j.molstruc.2020.128059>
- [17] Aktar BSK, Sicak Y, Tatar G, Emre EE. Synthesis of benzoyl hydrazones having 4-hydroxy-3, 5-dimethoxy phenyl ring, their biological activities, and molecular modeling studies on enzyme inhibition activities. *Turk J Chem.* 2022; 46(1): 236-252. <https://doi.org/10.3906/kim-2107-7>
- [18] Aktar BSK, Sicak Y, Tatar G, Emre OEE. Synthesis, antioxidant and some enzyme inhibition activities of new sulfonyl hydrazones and their molecular docking simulations. *Pharm Chem J.* 2022; 56(4): 559-569. <https://doi.org/10.1007/s11094-022-02674-3>
- [19] Hossain U, Das AK, Ghosh S, Sil PC. An overview on the role of bioactive  $\alpha$ -glucosidase inhibitors in ameliorating diabetic complications. *Food Chem Toxicol.* 2020; 145:111738. <https://doi.org/10.1016/j.fct.2020.111738>
- [20] Hedrington MS, Davis SN. Considerations when using alpha-glucosidase inhibitors in the treatment of type 2 diabetes. *Expert Opin Pharmacother.* 2019;20(18):2229-2235. <https://doi.org/10.1080/14656566.2019.1672660>
- [21] Dassault Systèmes BIOVIA, Discovery Studio Modeling Environment, Release 2019, San Diego: Dassault Systèmes, 2019.
- [22] Morris GM, Huey R, Lindstrom W, Sanner MF, Belew RK, Goodsell DS, vd. AutoDock4 and AutoDockTools4: Automated Docking with Selective Receptor Flexibility. *J Comput Chem.* 2009;30(16):2785-2791. <https://doi.org/10.1002/jcc.21256>